Journal of Advanced Zoology

ISSN: 0253-7214
Volume ***44*** *Issue* ***S-2 Year 2023*** *Page* ***1096:1109***

The Effect of Cinnamon versus Atorvastatin on the Submandibular Salivary Gland of Hypercholesterolemic Albino Rats (Histological, Immunohistochemical and Ultrastructural study)

Asmaa Ahmed Foad [(1)] Elham Fathy Mahmoud [(2)] Mervet Mohammed Hawwas [(3)] Abdel Nasser Mohammed Hashem El-Refai [(4)] Enas Hegazy [(5)]

1) PHD Faculty of Dentistry, Beni Suef University.
2) Professor of Oral Biology, Faculty of Dentistry, Suez Canal University.
3) Professor of Oral Biology, Faculty of Dentistry, Suez Canal University.
4) Professor of Oral Medicine, Faculty of Dentistry, Suez Canal University.
5) Assoc. Professor of Oral Biology, Faculty of Dentistry, Suez Canal University.

Corresponding Author:
Asmaa Ahmed Foad
Email address: *(asmaaahmedfoad14@gmail.com)*.

Article History
Received: 29 Aug 2023
Revised: 28 Sept 2023
Accepted: 07 Oct 2023

Abstract:

Background: Hypercholesterolemia refers to elevated cholesterol levels in the blood, and statin family compounds are essential synthetic medications for treating this condition. Plant extracts, such as cinnamon, were used to treat various diseases, researchs showing that cinnamon significantly reduces blood triglycerides and total cholesterol while increasing HDL cholesterol levels.

Objectives: The present study's goal was to compare the effect of Cinnamon versus Atorvastatin on the submandibular salivary gland of hypercholesterolemic albino rats.

***Materials and Methods*:** There were two groups of twenty-eight male albino rats. **(1) Control group:** rats were kept on a normal diet, **(2) Experimental groups**: Hypercholesterolemic group: rats fed with hypercholesterolemic rich diet for 4 months, Atorvastatin and Cinnamon groups: rats were given Atorvastatin tablets and Cinnamon powder at the beginning of the third month with a dose of 10 mg/kg BW. and 6mg \ Kg. B.W. respectively. Sections 5 mm thick of the submandibular salivary glands were examined histologically, ultra-structurally, and immunologically through assessment of anti-Caspase Ⅲ immune antibody.

Results: The group with high cholesterol showed marked degenerative changes in parenchymal elements of the submandibular salivary gland, while the Atorvastatin and Cinnamon groups showed a marked enhancing effect in the histological structure of the rat's submandibular gland.

Conclusion: Administration of Atorvastatin as a synthetic line of treatment for hypercholesterolemia positively affected submandibular gland tissue and the cholesterol level in the blood. As a natural herbal line of treatment Cinnamon enhanced the histological and ultrastructure picture of the submandibular gland, level of caspase III in addition to blood cholesterol levels in hypercholesteraemic rats.

Key Words: Submandibular Salivary Gland, Cinnamon, Atorvastatin, Hypercholesterolemia.

Introduction:

One of the lipids, cholesterol, is crucial for maintaining the fluidity and biophysical properties of cellular membranes by reducing permeability and boosting compactness. The development of the

embryo and fetus depends on cholesterol. In addition, cholesterol is a source of bioactive substances like steroid hormones, vitamin D, and bile acids, which in turn can control cellular metabolism and intracellular and extracellular communication **(Woollett et al.,2011).**

There are many ways to treat hypercholesterolemia, including herbal remedies or synthetic medications. The statins, which form a heterogeneous group and block the activity of HMG CoA reductase (hydroxy methyl glutaryl coenzyme A), an essential enzyme for the production of cholesterol, are among the most significant synthetic medications used to treat such medical disorders. As a result, statins are used globally to treat dyslipidemia **(Nayor and Vasan, 2016).**

Atorvastatin is a statin recommended for treating various dyslipidemias, including primary hyperlipidemia, mixed dyslipidemia in adults, hypertriglyceridemia, primary lipoproteinemia, homozygous familial hypercholesterolemia, and heterozygous familial hypercholesterolemia in adolescents **(Qiu et al.,2017).**

Asian countries often use traditional plant-based medicine, including Cinnamomum burmannii, which can lower blood sugar levels and potentially be anti-diabetic due to its high levels of cinnamaldehyde. Cinnamon's strong lipolytic activity affects lipid metabolism, preventing hypercholesterolemia and hypertriglyceridemia. Cinnamaldehyde, the most abundant compound in Ceylon cinnamon bark extracts, moderately inhibits bile acid binding, cholesterol micellization, and cholesterol esterase in vitro, potentially reducing cholesterol levels due to its role in bile acid production **(Heydarpour et al., 2020).**

Materials and Methods

The Faculty of Dentistry at Suez Canal University's Research Ethics Committee (REC) gave its approval for the current study with approval number (284/2020). The research was done on 28 male mature albino rats (according to sample size calculation). Twenty- eight male albino rats weighing between 200-250 gm each, were used in this study. The animals were separated into the following categories:

1- **Control group:** This group consisted of 7 rats. They were kept on a normal diet and received distilled water via a gastric tube for 4 months.

2- **Experimental groups:**

2. A Cholesterol-rich diet group: This group consisted of 7 rats and received a cholesterol-rich diet containing 1% cholesterol for 4 months **(Moubarak, 2008).**

2.B Cholesterol-rich diet + Atorvastatin group*:* This group consisted of 7 rats and were kept on a cholesterol-rich diet for 3 months, and Atorvastatin was started at the beginning of the fourth month in combination with a cholesterol diet at a dosage of 10 mg/kg body weight till the conclusion of the testing period **(Ulicna et al., 2012).**

2.C Cholesterol-rich diet + Cinnamon group: This group consisted of 7 rats that were fed a diet high in cholesterol for three months. Cinnamon was combined with cholesterol at the beginning of the fourth month, and each rat was given a dose of 6mg \ Kg. BW cinnamon powder **(Iqbal, 2016).**

- Blood samples were obtained from each rat at the beginning, after three months, and at the end of the experimental periods in all groups. Lipid profiles were assessed before induction of hypercholesterolemia, after induction of hypercholesterolemia (at the end of the third month), and after the trial period.

-Rats euthanized at the end of 4 months. They were euthanized by overdose inhalation of ether. After euthanization both right and left submandibular salivary gland specimens were collected,

and divided to accommodate histological, ultrastructural, and immunohistochemical demands.

- Dead experimental animals were disposed of by burning in the Animal Aching Unit of the Faculty of Medicine, Suez Canal University.

Results:

I- Biochemical Analysis:

- **Mean Plasma Cholesterol level before induction of hypercholesterolemia, all groups' results after the third month and the fourth month showed:** Plasma Cholesterol level showed the same level at all groups before induction of hypercholesterolemia and t-test showed insignificant statistical difference between groups.
- Mean plasma Cholesterol level after induction of hypercholesterolemia showed a lesser value in the control group compared to other groups.
- Compared to other groups, the average plasma cholesterol level in the cholesterol group significantly increased at the end of the fourth month.
- Compared to the Cholesterol group, the cholesterol + Atorvastatin group demonstrated a substantial drop; however, there was no difference between the Cholesterol+ Atorvastatin group and the Control group.
- Compared to the Cholesterol group, the Cholesterol+ Cinnamon group showed a considerable reduction, but the comparison between the Cholesterol + Cinnamon group and the control group revealed no discernible change **in Table (1)**.

Table (1): Mean Plasma Cholesterol levels of the different experiment groups.

	Before induction of hypercholesterolemia	**At the end of the third month**	**At the end of the fourth month**
Control	97.432	98.857	99.125
Cholesterol rich diet	97.28	165.542	233.525
Cholesterol + Atorvastatin	95.142	166.828	115.202
Cholesterol + Cinnamon	96.000	165.943	113.584

II- ***Histological*** **Results: (Figure.1)**.

1- Control group: Examination of H&E-stained sections revealed that submandibular gland's parenchyma consists of secretory end pieces and collecting ducts, with intercalated ducts having narrow lumens and cuboidal cells with basally located nuclei, and striated ducts consisting of columnar cells with centrally placed open-faced nuclei **(Fig. 1A).**

2- Cholesterol-rich diet group: Microscopic examination of a group of cells revealed a loss of normal acinar cell arrangement, disrupted boundaries, vacuolar degeneration, prominent chromatin, and abnormal mitosis. Intercalated duct cells showed abnormal architecture with ill-defined boundaries, while striated duct cells had ill-defined boundaries and complete loss of basal striations. Cytoplasm appeared degenerated, and most nuclei showed signs of necrosis with vacuolated cytoplasm. Granular convoluted tubules also showed a loss of normal architecture, indistinguishable boundaries, and necrotic cells **(Fig. 1B).**

3- Cholesterol-rich diet+ Atorvastatin: The group's histological examination revealed a return to typical acinar appearance and normal secretory cell arrangement into spherical-shaped acini. Some serous acini had ruptured cells, while some acinar cells lost their pyramidal shape and cellular boundaries. Intercalated duct showed normal cell boundaries with a narrow lumen **(Fig. 1C).** The study found granular convoluted tubules with normal histological structure, striated ducts with

returning normal cell boundaries, and basal striations **(Fig. 1D).**

4- **Cholesterol-rich diet + Cinnamon:** The gland's normal structural features were preserved in hematoxylin and eosin-stained sections, with a regular arrangement of secretory acini and ducts. The intercalated duct showed normal histological features, while striated duct cells had well-defined boundaries and basal striations. Some ducts retained secretion. The granular convoluted tubule had normal boundaries, tall columnar cells, and a wide lumen **(Fig. 1E).**

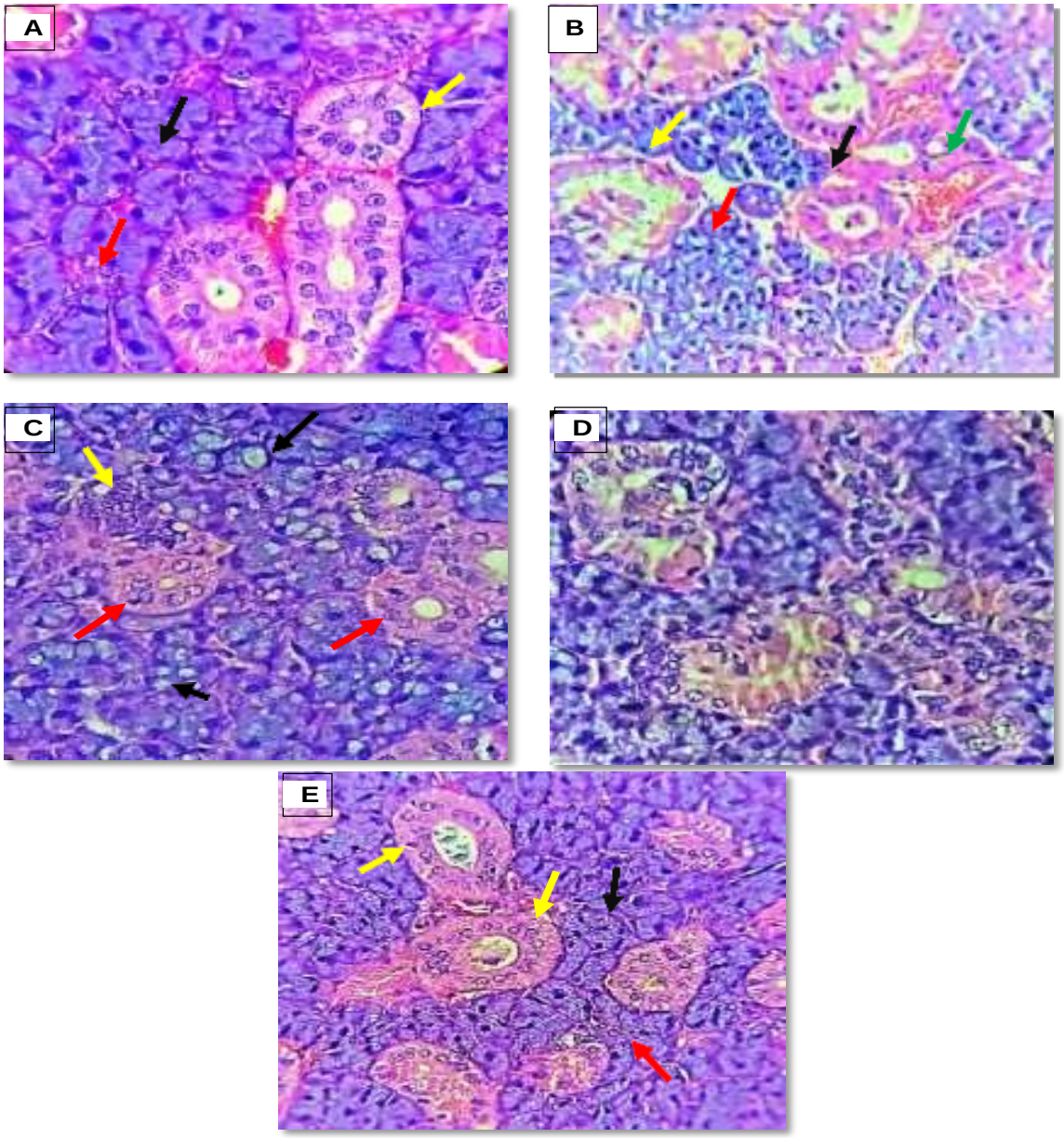

Fig. 1: (A) A photomicrograph of the control group showing serous acini (black arrow). Intercalated duct (red arrow), striated ducts (yellow arrow), **(B):** A photomicrograph of cholesterol group showing serous acini with vacuolated cytoplasm (red arrows), convoluted tubule with necrotic cells and wide lumen (yellow arrow). Vacuolated striated ducts with loss of basal striation (black arrows), dilated blood vessel congested with RBCs (green arrow), **(C):** A photomicrograph of atorvastatin treated group showing serous acini with cytoplasmic vacuoles (black arrows), intercalated duct (yellow arrow), striated ducts with basal striations (red arrows), **(D):** A photomicrograph of the same group showing granular convoluted tubule with normal cell boundaries (red arrows), and **(E):** A photomicrograph of cinnamon treated group showing spherical acini (black arrows), standard intercalated duct (red arrow), striated ducts with retained secretion (yellow arrows), convoluted granular tubule with tall columnar cells and cytoplasmic granules (green arrow) **(H & E, x 400, 640).**

Ⅲ- *Immunohistochemical* Results: (Figure.2)

- Regarding the qualitative analysis of color intensity immunoreaction to Caspase Ⅲ in rats fed with a normal diet for four months showed negative to weak immune reaction. While the Cholesterol rich diet group showed strong to moderate positive Immune reactivity and the mean of anti-caspase immune reaction in the submandibular salivary gland at the end of the fourth month showed a significant increase in the mean of anti-caspase immune reaction in the Cholesterol group in comparison with the other groups.
- Hypercholesterolemic rats treated with Atorvastatin tablets for 1 month revealed strong to moderate immuno-reactivity with insignificance between this group and the cholesterol group.
- Hypercholesterolemic rats treated with Cinnamon showed weak immune reaction to caspase Ⅲ antibody. A significant difference between this group and the cholesterol group and an insignificant difference with the control group **(Table 2).**

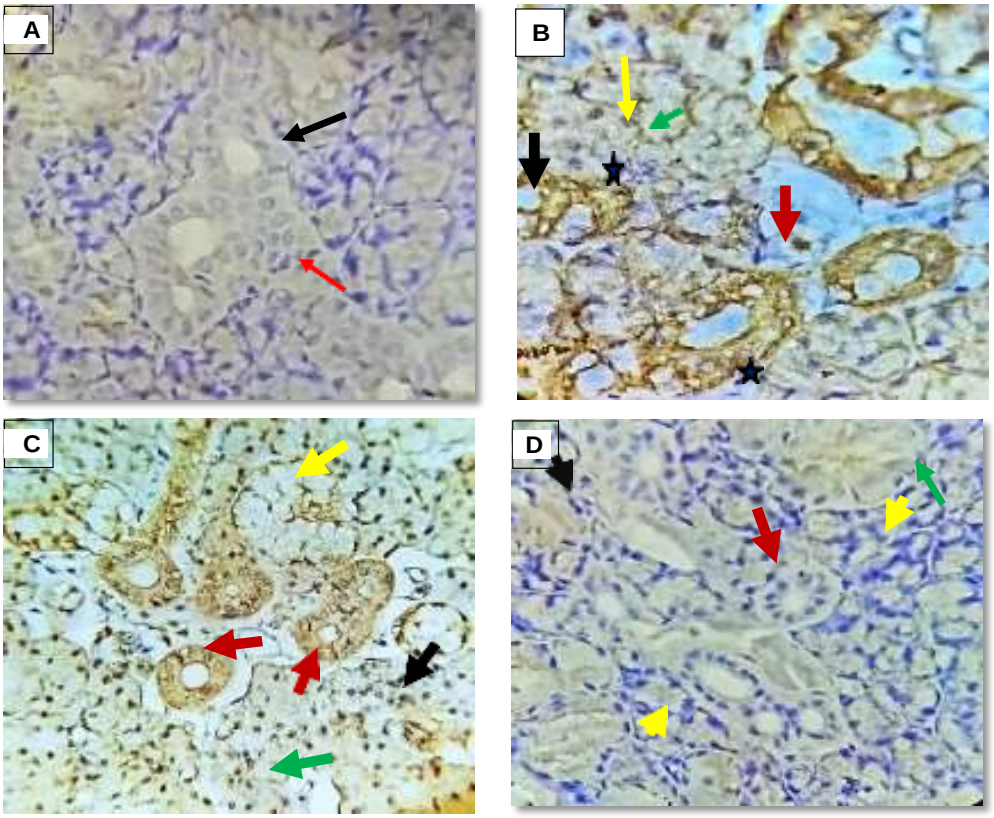

Fig. 2: (A): A photomicrograph of the control group showing negative to weak immune reaction in the cytoplasm of acinar cells. Duct cells of striated ducts (black arrow), intercalated ducts (red arrow). **(B):** A photomicrograph of the cholesterol group showing strong to moderate immune reaction at the basement membrane and cytoplasm of intercalated (black arrow) and striated duct cells (red arrow). **(C):** Photomicrograph of atorvastatin treated group showing strong to a moderate immune reaction in the cytoplasm and basement membrane of intercalated duct cells (black arrow) and striated duct cells (red arrow), moderate to weak immune reaction at acinar cells cytoplasm (green arrows). The granular duct showed a negative immune reaction (yellow arrow), and **(D):** A photomicrograph of cinnamon treated group showing negative to weak immune reaction in acinar cells cytoplasm and nuclei (yellow arrows). Negative immune reaction at the basement membrane and cytoplasm of intercalated (black arrow) and striated duct cells (red arrow). The granular convoluted tubule showed a weak reaction (green arrow) **(Caspase Ⅲ, x640).**

Table (2): Mean of submandibular salivary gland Caspase Ⅲ immune reaction of the different experiment groups.

	Mean	Std. Deviation	Std. Error	95% Confidence Interval Lower Bound	Upper Bound	Color Intensity Percentage
Control group	32.4324	8.757215	0.380829579	-1.369438919	0.745265922	5.07%
Cholesterol	129.5476	24.20065	0.492517234	-1.41101364	1.323880489	45.55%
Cholesterol + Atorvastatin	43.1716	7.398703	0.746366778	-2.515255232	1.629237545	15.18%
Cholesterol + Cinnamon	28.144	15.83386	0.661310698	-1.273396119	2.39878958	13.75%

Ⅳ- Transmission Electron Microscope Results:

1- Control Group

The submandibular salivary gland of a rat showed normal ultrastructural elements, with spherical acini with a central narrow lumen and pyramidal cells. Golgi bodies were found basally and laterally, and free ribosomes and lysosomes had different electron densities. The basal part of the cells contained rounded euchromatic nuclei surrounded by numerous mitochondria **(Fig. 3A).** The granular convoluted tubules were lined by tall columnar cells with large, rounded nuclei. Many well-circumscribed membrane-bound granules were observed **(Fig. 3B).**

2- Cholesterol-rich diet group

The study examined the submandibular salivary glands of a cholesterol-rich diet group, revealing serous secretory cells with atrophic changes. The acinar cells were pyramidal, irregular, and had cytoplasmic vacuolations. Some acini showed degeneration of cell organelles, mitochondrial loss, and widened intercellular junctions. The study also revealed a lack of interdigitation **(Fig. 3C).** The study revealed severe damage to granular convoluted tubules, with multiple cell vacuolization indicating damaged mitochondria, rough endoplasmic reticulum, and other organelles **(Fig. 3D).**

3- Cholesterol-Rich Diet + Atorvastatin Group

Electron microscopic examination of the submandibular salivary gland of the cholesterol-rich diet group treated by Atorvastatin showed relatively returning the normal ultrastructural elements. Serous acini of the rat's submandibular salivary gland of this group showed large pyramidal cells with almost rounded basally located nuclei. Cell membranes of the adjacent cells showed relative intercellular junctions, represented by numerous integrations as well as numerous desmosomes **(Fig. 3E).** Granular convoluted tubules were lined with columnar cells showing basally located nucleus; many cytoplasmic granules were seen **(Fig 3F)**.

4- Cholesterol Rich Diet + Cinnamon

Electron microscopic examination of the submandibular salivary gland of the cholesterol-rich diet group treated by Cinnamon showed the serous acini of the rat's submandibular salivary gland of this group with large pyramidal cells with an almost rounded basally located nucleus. **(Fig. 4G).** Granular convoluted tubules were lined with columnar cells showing a basally located nucleus. Cells are arranged around the lumen, which contains liquid stagnation. Many large-sized cytoplasmic granules and newly formed ones were seen. Some newly formed mitochondria were seen, but some of them were bursed around **(Fig. 4H)**.

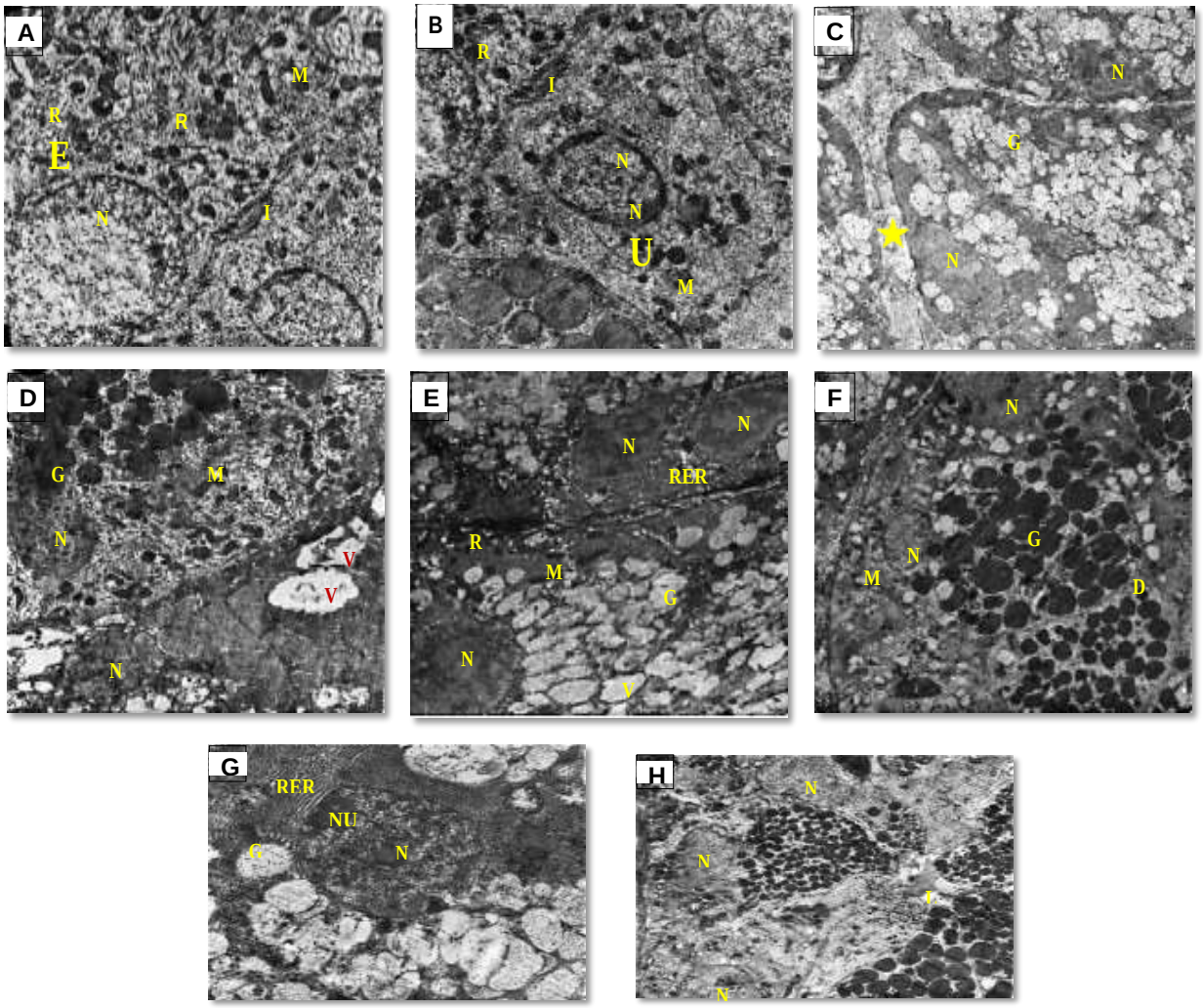

Fig. 3: (A) An electron micrograph of the control group showing a serous secretory cell with nucleus (N), rough endoplasmic reticulum (RE), Mitochondria (M), and free ribosomes (R). Lateral interdigitation (I) was noticed **(Uranyl acetate & lead citrate x12000). (B):** Electron micrograph of the same group showing granular convoluted tubules of rounded nuclei (N) and condensed nucleolus (NU). Free ribosomes (R) and mitochondria (M). Lateral interdigitations were observed (I) **(Uranyl acetate & lead citrate x12000). (C):** Electron micrograph of cholesterol group showing acinar cells, pyramidal with irregular shrunken nuclei (N), and multiple electro-lucent secretory granules (G) were noticed. Large and small cytoplasmic vacuoles **(Arrows).** Widened intercellular junctions (Stars) **(Uranyl acetate & lead citrate x5000). (D):** higher magnification of granular convoluted tubule of cholesterol group with irregular degenerated nucleus (N) and ruptured mitochondria (M), cytoplasmic vacuoles (V), and pleomorphic granules **(G) (Uranyl acetate & lead citrate x8000). (E):** An electron micrograph of the atorvastatin-treated group showing serous acinar cells with rounded nuclei (N), mitochondria (M), free ribosomes (R), and rough endoplasmic reticulum (RER). Cytoplasmic vacuoles (V) and secretory granules were noticed **(**G). Cell membranes of the adjacent cells showed numerous desmosomes **(arrows) (Uranyl acetate & lead citrate x8000). (F):** An electron micrograph of the atorvastatin-treated group showing granular convoluted duct cells with rounded basally located nuclei (N). Many cytoplasmic granules (G). desmosomal junctions (D), some bursed mitochondria were also observed (M). **(Uranyl acetate & lead citrate x5000). (G):** An electron micrograph of serous acini of cinnamon treated group showing a serous acinar cell with rounded nucleus (N), prominent nucleolus (NU), Rough endoplasmic reticulum **(**RER) and cytoplasmic granules (G) **(Uranyl acetate & lead citrate x12000). (H):** An electron micrograph of cinnamon treated group showing the granular convoluted tubules with basal nucleus (N). Narrow lumen with liquid stagnation (L). many cytoplasmic granules (G). lateral interdigitation (Arrows) (Uranyl acetate & lead citrate x5000) was noticed**.**

Discussion:

According to prior study findings published by **Khosla and Sundram (1996)**, who employed albino rats fed on various amounts and kinds of fats, feeding albino rats a high-fat meal including cholesterol crystals, they produced hypercholesterolemia in the diet group high in cholesterol.

The current investigation found that adding supplements to a diet rich in cholesterol was sufficient to result in hyperlipidemia. **Arafa (2005)**;**Varsha et al. (2010)**, and **Iqbal and Mudassar (2015)** published similar findings demonstrating increased blood lipid profile values in rats and rabbits on a high-cholesterol diet.

The submandibular salivary gland of albino rats given a high-fat diet for four months was examined histologically and ultrastructural to determine how the high-fat diet affected the gland's histological structure and led to the loss of the typical morphology of acinar cells.

It was discovered that a high-fat diet causes significant changes in the parotid salivary gland, leading to lipid buildup and inflammatory responses, potentially limiting oxygen and food molecules, and negatively impacting cell function and survival **(Raal et al., 1997; Pisiriciler et al., 2019).**

The study suggests that intracellular lipids cause vacuoles, which may be due to degenerative changes in secretory cells. This aligns with previous research suggesting that high-fat diets cause lipid accumulation in secretory cells. Salivary glands accumulate lipid droplets, causing pressure on acini boundaries and resulting in eroded and deformed structures **(Jang et al., 2002).**

On the ultrastructural evaluation scale. It was proposed that cytoplasmic vacuolization is a physiological adaptation to limit harm, starting with tiny vesicles fused into larger vacuoles. Following hypotonic shock, cells' distended mitochondria give them a vacuolated appearance, impacting the endoplasmic reticulum and Golgi apparatus **(Henics and Wheatley, 1999).**

Rats fed a high-fat diet show significant changes in their submandibular salivary gland, resulting from lipid droplet pressure and increased salivary secretion. This is linked to glandular dysfunction and abnormal secretory duct degeneration **(Moubarak, 2008).**

It was explained that dilated striated ducts and stagnate excretion may be due to mitochondrial injury, ATP depletion, membrane pump failure, and biosynthesis failure. This lack of energy leads to ductal dilatation and obstruction, resulting in the transfer of secretions by cells **(Starkov and Wallace, 2002).**

Red blood cells were found in dilated blood arteries in a group with hypercholesterolemia, consistent with previous studies showing cellular infiltration and dilated blood channels congested with red blood cells in hypercholesterolemic rats, possibly due to an inflammatory response to improve blood supply to degeneration areas **(Pisiriciler et al., 2009).**

Ultrastructural analysis revealed dilated rough endoplasmic reticulum (RER) in some acini, with severe organelle degeneration and weak intercellular connections. This aligns with previous studies showing that a lipid-rich diet in rats leads to recessed, compressed nuclei with little or no euchromatin, indicating a potential link between lipid-rich diets and acinar cell dysfunction **(Selim, 2013).**

The marked dilatation of the rough endoplasmic reticulum (RER) was also explained by **An, Wang et al. (2005),** who confirmed that the RER's enlargement is related to the cellular condition that occurs before apoptotic manifestations.

Electron microscopy research indicates that the packing of mitochondria between plasma membrane basal infoldings causes striated duct cell basal striations, which could be lost due to mitochondrial damage caused by oxidative stress **(Young and Van, 1979).**

The study's immunohistochemical results confirmed the findings in the hypercholesterolemic group, with caspase Ⅲ antibodies showing strong to moderate positive reactions to activated caspase Ⅲ in acinar and ductal cells, connective tissue cells, and endothelial cells.

Research suggests that strong to moderate immune reactivity in this population may be due to the activation of "death domain" receptors, such as TNFR-1 or FAS, by cytokines, possibly due to hypercholesterolemia **(Alikhani et al., 2005).**

The study suggests that hypercholesterolemia can lead to increased oxidative stress, causing excessive reactive oxygen species (ROS) development and severe oxidation of cell lipids, proteins, and DNA. This, through caspase III activation, results in apoptosis, a common pathogenic outcome in hypercholesterolemia **(Riedl and Shi, 2004).**

On the other hand, **Jang, Shin et al. (2002)** added that caspase Ⅲ has several cellular targets, and upon activation, caspase III results in morphologic characteristics of apoptosis.

The study involved albino rats fed a high-fat diet for three months, who were given a month of treatment with 10 mg/kg BW Atorvastatin tablets, a favored clinical lipid-regulating medication.

AL-Rawi (2007) reported that in patients with hyperlipidemia, atorvastatin effectively reduces abnormal blood cholesterol levels, inhibits the development of atherosclerosis, and reduces clinical cardiovascular events.

In comparison to the cholesterol group, this group's biochemical data indicated a substantial drop in total cholesterol, LDL, and HDL levels.

Studies have shown that statins inhibit HMG-CoA reductase, lowering cholesterol levels and increasing protease activity. This leads to increased sterol regulatory element binding protein (SREBP) entry into the endoplasmic reticulum, regulating the amount of circulating LDL **(Sehayek et al., 1994).**

Researchers have also shown that statins reduce LDL by blocking the liver from generating the LDL receptors known as apolipoprotein B-100. When LDL receptors are not working in persons with hypercholesterolemia, atorvastatin can reduce LDL **(Gaw et al., 1993; Kostner et al., 1989; Marais et al., 1997; Raal et al., 1997).**

In the present experiment, histological and ultrastructural examination of hypercholesterolemic r34.s treated with Atorvastatin showed that the normal structural features of the gland were almost treated to their normal features.

The return of typical acinar appearance with its histological features in this group was explained by **Laufs, La Fata et al. (1998)**, Who claimed that endothelial dysfunction is a precursor to atherosclerotic lesions, which are brought on by high cholesterol. The ability of endothelial cells to generate nitrous oxide (NO), which controls the endothelium's anti-atherosclerotic activity, is decreased by hypercholesterolemia.

Previous findings were reported by **Wagner, Köhler et al. (2000)**, who proposed that statins change the NO-/ O2- balance by stopping endothelial cells from producing O2, which then allows endothelial cells to function again.

Histological and ultrastructural examination of this group showed the return of the Intercalated, striated, and excretory ducts to their normal histological features.

The study supports previous research indicating statins improve blood flow control and lipid profile modification, leading to increased endothelium-dependent vasodilation, tissue repair, and the development of new blood vessels **(Pan et al., 2022).**

Histological analysis revealed dilated granular convoluted tubules in the same group, with cytoplasmic vacuolar degeneration in some. However, cell borders and nuclei were only slightly normal in other granular tubules, attributed to studies showing that statins reduce cholesterol and coenzyme Q10 production in hypercholesterolemia patients **(Diebold et al., 1994; Nakahara et al., 1998; Satoh and Ichihara, 2000; Berthold et al., 2006).**

Vascular degenerative signs of the granular convoluted tubule and some acinar cells may be because of what **Kumar (2007)** showed that treatment with atorvastatin caused pancreatic acinar degeneration in hyperlipidemic rats in various degrees, resulting in the loss of their normal architecture and empty spaces between the pancreatic acini. Acinar cells might have unclear cell borders. It clarifies the implications of the poor histology data.

The study found that high-fat diet rats treated with Atorvastatin showed strong to moderate immunoreaction against caspase Ⅲ, consistent with **Chen, Zhu et al. (2014)**. who found that atorvastatin improved left ventricular function, reduced infarct size, and decreased cell apoptosis in rats with experimental acute myocardial infarction.

The Bcl-2 family in the endoplasmic reticulum regulates various signaling pathways and cell viability. Anti-apoptotic proteins like Bcl-2 may explain their moderate to poor response to various apoptosis inducers **(Anilkumar and Prehn, 2014).**

It is now regular practice to employ plant extracts to treat various illnesses. Additionally, many plant materials are used as supplements. In this research, albino rats fed a high-fat diet for 4 months were treated with 6 mg/kg. BW cinnamon powder.

Using 6 mg cinnamon powder in agreement with **Khan, Safdar et al. (2003)** findings, they discovered that cinnamon bark's potent lipolytic action helped type 2 diabetic individuals lower their free fatty acid levels and manage their total cholesterol and triglyceride levels at varied dosages. This proves that cinnamon powder effectively avoids hyperlipidemia's elevated lipid profile levels.

The study found that when cinnamon powder was administered to hypercholesterolemic rats, plasma cholesterol and LDL levels decreased by 54%, LDL decreased by 211 mg/dl to 61 mg/dl, and HDL increased dramatically from 36 mg/dl to 63 mg/dl **(Abd El-Rahman et al., 2010).**

In addition, **Khan, Safdar et al. (2003)** revealed that cinnamon medication directly impacts how lipids are metabolized. Thanks to its potent lipolytic action, cinnamon protects against hypercholesterolemia and hypertriglyceridemia and decreases levels of free fatty acids and TG.

The ultrastructural analysis reveals columnar cells bordering striated channels, with radially distributed mitochondria and complex infoldings. Cinnamon's active ingredient controlling mitochondrial permeability may contribute to the observed advancement in mitochondrial structure **(Kassaee et al., 2017).**

Similarly, **(Mohammed and Abdel Fattah 2018)** reported that by preventing the mitochondrial permeability transition, cinnamon polyphenols reduced oxygen-glucose deprivation, decreasing the inner mitochondrial membrane potential and causing cell enlargement.

In hypercholesterolemic rats treated with Cinnamon, immunohistochemical analysis with caspase III revealed a negative to mild immunoreaction that was shown in acini and duct cells which may be due to natural cell death **(Olney et al., 2002).**

Hecht et al. (2000) evaluated the development of the mouse submandibular organ during its transition from the perinatal organize to the developed grown-up arrange, even though death of salivary organ cells has been demonstrated in a few obsessional settings. They suggested that physiological apoptosis may be partially responsible for the demise of Sort I cells and the decline in submandibular positivity of intercalated channels in adult rats.

Conclusion: Hypercholesterolemia severely affects the structure of the salivary glands to different degrees. Administration of Atorvastatin as a synthetic line of treatment for hypercholesterolemia positively affected submandibular gland tissue and the cholesterol level in the blood. As a natural herbal line of treatment Cinnamon enhanced the histological and ultrastructure picture of the submandibular gland, level of caspase III in addition to blood cholesterol levels in hypercholesteraemic rats.

References:

Abd El-Rahman, S. N., A. M. Abdel-Haleem and H. M. A. Mudhaffar (2010). "Anti-diabetic effect of cinnamon powder and aqueous extract on rats." International Journal of Food, Nutrition and Public Health **3**(2): 183.

AL-Rawi, M. M. (2007). "Efficacy of oat bran (Avena sativa L.) in comparison with atorvastatin in the treatment of hypercholesterolemia in albino rat liver." The Egyptian Journal of Hospital Medicine **29**(1): 511-521.

Alikhani, Z., M. Alikhani, C. M. Boyd, K. Nagao, P. C. Trackman and D. T. Graves (2005). "Advanced glycation end products enhance expression of pro-apoptotic genes and stimulate fibroblast apoptosis through cytoplasmic and mitochondrial pathways." Journal of Biological Chemistry **280**(13): 12087-12095.

An, W. W., M. w. Wang, S. i. Tashiro, S. Onodera and I. Takashi (2005). "Mitogen-activated protein kinase-dependent apoptosis in norcan-tharidin-treated A375-S2 cells is proceeded by the activation of protein kinase C." Chinese Medical Journal **118**(03): 198-203.

Anilkumar, U. and J. H. Prehn (2014). "Anti-apoptotic BCL-2 family proteins in acute neural injury." Front Cell Neurosci **8**: 281.

Arafa, H. M. (2005). "Curcumin attenuates diet-induced hypercholesterolemia in rats." Med Sci Monit **11**(7): BR228-234.

Berthold, H. K., S. Unverdorben, R. Degenhardt, M. Bulitta and I. Gouni-Berthold (2006). "Effect of policosanol on lipid levels among patients with hypercholesterolemia or combined hyperlipidemia: a randomized controlled trial." Jama **295**(19): 2262-2269.

Chen, T. L., G. L. Zhu, X. L. He, J. A. Wang, Y. Wang and G. A. Qi (2014). "Short-term pretreatment with atorvastatin attenuates left ventricular dysfunction, reduces infarct size and apoptosis in acute myocardial infarction rats." Int J Clin Exp Med **7**(12): 4799-4808.

Diebold, B. A., N. V. Bhagavan and R. J. Guillory (1994). "Influences of lovastatin administration on the respiratory burst of leukocytes and the phosphorylation potential of mitochondria in guinea pigs." Biochim Biophys Acta **1200**(2): 100-108.

Gaw, A., C. J. Packard, E. F. Murray, G. M. Lindsay, B. A. Griffin, M. J. Caslake, B. D. Vallance, A. R. Lorimer and J. Shepherd (1993). "Effects of simvastatin on apoB metabolism and LDL subfraction distribution." Arterioscler Thromb **13**(2): 170-189.

Hecht, R., M. Connelly, L. Marchetti, W. D. Ball and A. R. Hand (2000). "Cell death during development of intercalated ducts in the rat submandibular gland." Anat Rec **258**(4): 349-358.

Henics, T. and D. N. Wheatley (1999). "Cytoplasmic vacuolation, adaptation, and cell death: a view on new perspectives and features." Biol Cell **91**(7): 485-498.

Heydarpour, F., N. Hemati, A. Hadi, S. Moradi, E. Mohammadi and M. H. Farzaei (2020). "Effects of cinnamon on controlling metabolic parameters of polycystic ovary syndrome: A systematic review and meta-analysis." J Ethnopharmacol **254**: 112741.

Iqbal, Z., T. Ashraf, A. A. Khan, R. Hussain and M. Mudassar (2016). "Antihyperlipidemic efficacy of cinnamon in albino rats." Asian J Agri Biol **4**(1): 8-16.

IQBAL, Z., K. IQBAL and M. MUDASSAR (2015). "HEPATOPROTECTIVE EFFECT OF CINNAMON ON CHOLESTEROL INDUCED FATTY CHANGES IN ALBINO RATS." Isra Medical Journal **7**(4).

Ismail, N. S. (2014). "Protective effects of aqueous extracts of cinnamon and ginger herbs against obesity and diabetes in obese diabetic rat." World Journal of Dairy & Food Sciences **9**(2): 145-153.

Jang, M. H., M. C. Shin, H. S. Shin, K. H. Kim, H. J. Park, E. H. Kim and C. J. Kim (2002). "Alcohol induces apoptosis in TM3 mouse Leydig cells via bax-dependent caspase-3 activation." Eur J Pharmacol **449**(1-2): 39-45.

Kassaee, S. M., M. T. Goodarzi and E. A. Oshaghi (2017). "Renoprotective Effects of Trigonella foenum and Cinnamon on Type 2 Diabetic Rats." Avicenna Journal of Medical Biochemistry **5**(1): 17-21.

Khan, A., M. Safdar, M. M. Ali Khan, K. N. Khattak and R. A. Anderson (2003). "Cinnamon improves glucose and lipids of people with type 2 diabetes." Diabetes Care **26**(12): 3215-3218.

Khosla, P. and K. Sundram (1996). "Effects of dietary fatty acid composition on plasma cholesterol." Prog Lipid Res **35**(2): 93-132.

Kostner, G. M., D. Gavish, B. Leopold, K. Bolzano, M. S. Weintraub and J. L. Breslow (1989). "HMG CoA reductase inhibitors lower LDL cholesterol without reducing Lp (a) levels." Circulation **80**(5): 1313-1319.

Kumar, S. (2007). "Caspase function in programmed cell death." Cell Death Differ **14**(1): 32-43.

Laufs, U., V. La Fata, J. Plutzky and J. K. Liao (1998). "Upregulation of endothelial nitric oxide synthase by HMG CoA reductase inhibitors." Circulation **97**(12): 1129-1135.

Marais, A. D., R. P. Naoumova, J. C. Firth, C. Penny, C. K. Neuwirth and G. R. Thompson (1997). "Decreased production of low-density lipoprotein by atorvastatin after apheresis in homozygous familial hypercholesterolemia." J Lipid Res **38**(10): 2071-2078.

Mariee, A. D., G. M. Abd-Allah and H. A. El-Beshbishy (2012). "Protective effect of dietary flavonoid quercetin against lipemic-oxidative hepatic injury in hypercholesterolemic rats." Pharm Biol **50**(8): 1019-1025.

Mohammed, H. A. and D. M. Abdel Fattah (2018). "Hypolipidemic and hypoglycemic effect of cinnamon extract in high-fat diet-fed rats." Zagazig Veterinary Journal **46**(2): 160-167.

Moubarak, R. (2008). "The effect of hypercholesterolemia on the rat parotid salivary gland (histopathological and immunohistochemical study)." Cairo Dental Journal **24**(1): 19-28.

Nakahara, K., M. Kuriyama, Y. Sonoda, H. Yoshidome, H. Nakagawa, J. Fujiyama, I. Higuchi and M. Osame (1998). "Myopathy induced by HMG-CoA reductase inhibitors in rabbits: a pathological, electrophysiological, and biochemical study." Toxicol Appl Pharmacol **152**(1): 99-106.

Nayor, M. and R. S. Vasan (2016). "Recent Update to the US Cholesterol Treatment Guidelines: A Comparison With International Guidelines." Circulation **133**(18): 1795-1806.

Olney, J. W., T. Tenkova, K. Dikranian, L. J. Muglia, W. J. Jermakowicz, C. D'Sa and K. A. Roth (2002). "Ethanol-induced caspase-3 activation in the in vivo developing mouse brain." Neurobiol Dis **9**(2): 205-219.

Pan, E., S. J. Nielsen, A. Mennander, E. Bjorklund, A. Martinsson, M. Lindgren, E. C. Hansson, A. Pivodic and A. Jeppsson (2022). "Statins for secondary prevention and major adverse events after coronary artery bypass grafting." J Thorac Cardiovasc Surg **164**(6): 1875-1886 e1874.

Pışırıcıler, R., E. Çalişka-Ak, E. Emeklı-Alturfan, A. Yarat and Y. Canberk (2009). "Impact of Experimental Hyperlipidemia on Histology of Major Salivary Glands." Medical Journal of Trakya University/Trakya Universitesi Tip Fakultesi Dergisi **26**(4).

Qiu, S., W. Zhuo, C. Sun, Z. Su, A. Yan and L. Shen (2017). "Effects of atorvastatin on chronic subdural hematoma: A systematic review." Medicine (Baltimore) **96**(26): e7290.

Raal, F. J., G. J. Pilcher, D. R. Illingworth, A. S. Pappu, E. A. Stein, P. Laskarzewski, Y. B. Mitchel and M. R. Melino (1997). "Expanded-dose simvastatin is effective in homozygous familial hypercholesterolemia." Atherosclerosis **135**(2): 249-256.

Redman, R. S. (2008). "On approaches to the functional restoration of salivary glands damaged by radiation therapy for head and neck cancer, with a review of related aspects of salivary gland morphology and development." Biotech Histochem **83**(3-4): 103-130.

Riedl, S. J. and Y. Shi (2004). "Molecular mechanisms of caspase regulation during apoptosis." Nat Rev Mol Cell Biol **5**(11): 897-907.

Satoh, K. and K. Ichihara (2000). "Lipophilic HMG-CoA reductase inhibitors increase myocardial stunning in dogs." J Cardiovasc Pharmacol **35**(2): 256-262.

Sehayek, E., E. Butbul, R. Avner, H. Levkovitz and S. Eisenberg (1994). "Enhanced cellular metabolism of very low-density lipoprotein by simvastatin. A novel mechanism of action of HMG-CoA reductase inhibitors." European journal of clinical investigation **24**(3): 173-178.

Selim, S. A. (2013). "The effect of high-fat diet-induced obesity on the parotid gland of adult male albino rats: histological and immunohistochemical study." Egyptian Journal of Histology **36**(4): 772-780.

Starkov, A. A. and K. B. Wallace (2002). "Structural determinants of fluorochemical-induced mitochondrial dysfunction." Toxicol Sci **66**(2): 244-252.

Tenkova, T., C. Young, K. Dikranian, J. Labruyere and J. W. Olney (2003). "Ethanol-induced apoptosis in the developing visual system during synaptogenesis." Invest Ophthalmol Vis Sci **44**(7): 2809-2817.

Ulicna, O., O. Vancova, I. Waczulikova, P. Bozek, L. Sikurova, V. Bada and J. Kucharska (2012). "Liver mitochondrial respiratory function and coenzyme Q content in rats on a hypercholesterolemic diet treated with atorvastatin." Physiol Res **61**(2): 185-193.

Varsha, D., S. Shubhangi, P. Mangesh and N. Naikwade (2010). "Antihyperlipidemic activity of Cinnamomum tamala Nees. on high cholesterol diet induced hyperlipidemia." International Journal of PharmTech Research **2**(4): 2517-2521.

Wagner, A. H., T. Köhler, U. Rückschloss, I. Just and M. Hecker (2000). "Improvement of nitric oxide–dependent vasodilatation by HMG-CoA reductase inhibitors through attenuation of endothelial superoxide anion formation." Arteriosclerosis, thrombosis, and vascular biology **20**(1): 61-69.

Woollett, L. A. (2011). "Review: Transport of maternal cholesterol to the fetal circulation." Placenta **32 Suppl 2**(0 2): S218-221.

Young, J. A. and E. W. Van Lennep (1979). Transport in salivary and salt glands. Transport organs, Springer**:** 563-692.